Building Simulation 2005

Ninth International IBPSA Conference
Montréal, Canada
August 15-18, 2005

HOLISTIC RADIATION MODELLING WITH A FAST SIMPLIFIED RADIOSITY ALGORITHM

Darren Robinson[1] and Andrew Stone[2]
[1]Solar Energy and Building Physics Laboratory, Swiss Federal Institute of Technology, CH-1015 Lausanne, Switzerland. E: darren.robinson@epfl.ch W: http://leso.epfl.ch
[2]BDSP Partnership, Summit House, 27 Sale Place, London W2 1YR.

ABSTRACT

The radiant external environment may be described by two hemispheres, above and below the horizontal plane, which are discretised into patches of known solid angle. Occlusions to these patches may be combined and represented as some patch fraction for which the radiant characteristics are defined by the dominant occlusion. By solving for radiant exchanges between each surface in a scene and its associated (un)occluded patches, we have a simplified radiosity algorithm (SRA). This paper describes the application of this SRA to solve for predictions of (i) solar radiation, (ii) interior daylight and (iii) longwave radiation. Comparisons with a ray tracing program show that accurate results are achieved at a computational cost several orders of magnitude lower.

INTRODUCTION

Around half of the global population is now urbanised (in more developed countries the proportion is around three quarters) and this figure is forecast to increase by over 10% by 2030 (Population reference bureau, 2005). With the need to reduce greenhouse gas emissions from buildings becoming more pressing, so the application of building simulation tools to inform this process is likely to increase and the majority of these studies will address buildings in urban settings. It is therefore important that predictions from building simulation programs are sensitive to aspects of the urban context which can have reasonably significant impacts upon energy demands. Examples include (i) obstructions due to the sky vault and their associated impact on visible, short and long wave radiation exchange; (ii) modifications of meso-scale atmospheric flows, radiation and evapo(transpi)ration balances as well as anthropogenic gains, with consequent differences in temperature (both dry and wet bulb) recorded at climate stations; (iii) both meso-scale and local effects on wind pressure.

This paper considers the first of these domains of influence: radiation exchange.

SOLAR RADIATION

For some set of p sky patches, each of which subtends a solid angle Φ (Sr) and has radiance R ($Wm^{-2}Sr^{-1}$) then, given the mean angle of incidence ξ (radians) between the patch and our receiving plane together with the proportion of the patch that can be seen σ ($0 \le \sigma \le 1$), we have the following general solution for direct sky irradiance (Wm^{-2}), after Robinson and Stone (2004a):

$$I_{d\beta} = \sum_{i=1}^{p} \left(R\Phi\sigma\cos\xi \right)_i \quad \text{…[1]}$$

The radiance of the ith patch is given by [2]:

$$R_i = \ell v_i \, I_{dh} \Big/ \sum_{j=1}^{p} \left(\ell v \Phi \sin\bar{\gamma} \right)_j \quad \text{…[2]}$$

in which, after Perez et al (1993), the relative luminance of an arbitrary sky point ℓv is a function of the zenith angle of the considered sky point Z and the angle between this point and the sun θ ($\ell v = f(Z,\theta)$). The solid angle Φ is given by an expression due to Tregenza (1993), for discretisation schemes similar to his 145 patch sky and $\bar{\gamma}$ is the mean altitude of a given sky patch.

Now for radiation from (part) occluded patches $I_{\rho\beta}$ is also given by [1] but now summing to $2p$ patches (for two vaults), with the view factor depending on obstructions (rather than sky) and the corresponding radiance R [3] defined by the dominant occlusion (*): $I_{\rho\beta} = \sum_{i=1}^{2p} \left(R^* \Phi \omega \cos\xi \right)_i$.

$$R = \left(I_{b\xi} + \sum_{i=1}^{p} \left(R\Phi\sigma\cos\xi \right)_i + \sum_{j=1}^{2p} \left(R^*\Phi\omega\cos\xi \right)_j \right) \rho \Big/ \pi \quad \text{…[3]}$$

The terms in brackets correspond to contributions from the sun, sky and external obstructions (assuming Lambertian characteristics) respectively.

A set of simultaneous equations describing surface irradiance prediction for an entire external scene can be formulated into a matrix and solved by inversion for infinite reflections (Appendix 1) or by iteration (e.q. Gauss-Seidel) for finite reflections.

Solution of [3] requires that sky (σ) and obstruction (ω) view factors are known, as well as the mean incident beam irradiance at angle of incidence ξ ($I_{b\xi}$), which itself requires that the fraction of each

surface that is insolated be known. An efficient solution to this problem is based on computer rendering. For obstruction view factors, views encapsulating the hemisphere are rendered from each surface centroid, with every surface having a unique colour[1]. Each pixel is translated into angular coordinates to identify the corresponding patch as well as the angle of incidence. For sky view factors then, $\Phi\sigma\cos\xi$ is treated as a single quantity obtained by numerical integration of $\cos\xi \cdot d\Phi$ across each sky patch. Likewise for $\Phi\omega\cos\xi$, for which the dominant occluding surface is that which provides the greatest contribution. A similar process is repeated for solar visibility fractions for each surface, for which a constant size scene is rendered from the sun position. The ratio of the number of pixels that can be seen of each surface to those that would be visible if each surface was unobstructed defines the visibility fraction Ψ for time t so that the incident beam irradiance $I_{b\xi}$ is $I_{bn}\psi_t\cos\xi$.

Hourly results from this model, from near the base of both north and south sides at the centre of a hypothetical canyon at Kew, UK, are compared with predictions from RADIANCE (in conjunction with the module Gendaylit to use the same sky luminance/radiance distribution as that of the SRA) - Figure 1. The increased scatter observed in the south facing results is due to errors in interpolating solar visibility fractions – hourly solar views are only rendered for the central day of each month. Values for the same hours on other days are calculated using two dimensional three-point Lagrangian interpolation. With a diminished solar influence, the agreement between the SRA and RADIANCE is excellent for the north surface (shown below in Figure 1). Invoking RADIANCE's rtrace function with moderately accurate settings, the annual dataset for this single surface comparison takes *c*.five orders of magnitude longer to produce than that using the SRA. This relative difference is increased when solving for multiple surfaces, since the SRA solves for these simultaneously.

Note that by multiplying the numerator of [2] and the first bracketed term in [3] by diffuse and beam luminous efficacy respectively (e.g. using the Perez et al model (1990)), so that $R_{i,j}$ becomes $L_{i,j}$, we have an external illuminance solution. Furthermore, if we define a global distribution and sum for all daylight hours (so that we have units of $Whm^{-2}Sr^{-1}$) then we have a rapid solution for annual irradiation, or indeed mean illuminance ($lm.m^{-2}Sr^{-1}$) by dividing by the number of daylight hours, and these results may be conveniently presented by false colouring surfaces within some 3D model. The use of this technique in conjunction with RADIANCE (Robinson and Stone, 2004b) suggests that the errors involved with not solving for beam irradiation explicitly are reasonably modest for such aggregated results. This technique can therefore be used to produce the urban irradiation histograms of Compagnon (2004), to help with identifying the proportion of built surface for which solar technologies may be viable, at a considerable computational saving.

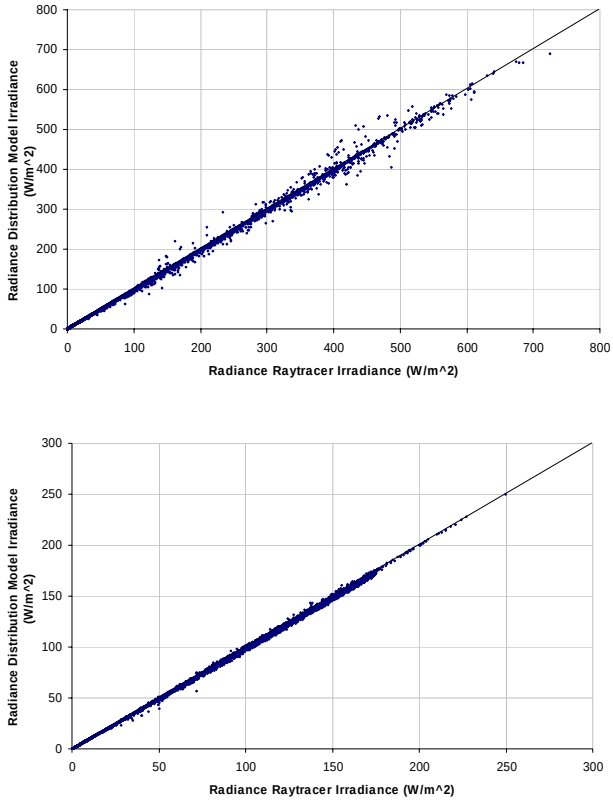

Figure 1 Hourly global irradiance incident on both south (above) and north (below) facing surfaces opposing diffusely reflecting obstructions: comparisons with RADIANCE simulation results, for Kew (UK), 1967.

DAYLIGHT

Given a sky patch luminance L, together with some glazing transmittance τ, the illuminance due to the sky at a point within a room is given by [4]:

$$E_s = \sum_{i=1}^{p} \left(L\Phi\sigma\tau\cos\xi\right)_i \qquad \ldots[4]$$

In this case however, our sky patch view factor must consider self-obstructions due to the surfaces

[1]starting at one end of the *r,g,b* scale for the first surface and cycling through towards the end of this scale, so that excepting the background colour, up to 256^3-1 unique surface identifiers are available – more than is likely to be needed for our purposes.

that bound the room φ and external obstructions ω, so that our sky patch view factor $\sigma_i = 1 - \varphi_i - \omega_i$.

The interesting issue here is how to determine the relevant view factors. For this we produce additional renderings from each calculation point, with internal surfaces having a consistent colour so that they can be ignored – effectively creating an image mask. The result for a simple problem in stereographic projection is shown in Figure 2. By processing the information at each pixel, we have the parameters of interest. The cost of these additional renderings is taken to be reasonable, since in this application we are interested in illuminance prediction at discrete points, as opposed to continuous distributions, to inform lighting control actions.

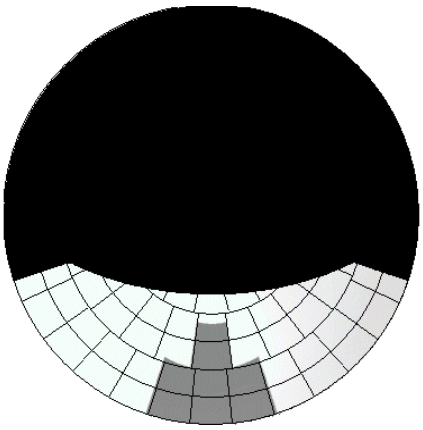

Figure 2 View from an internal calculation point to external light sources, masked due to self obstructions from opaque internal surfaces.

The contribution due to obstructions is solved simply by substituting ω into [4], using [3] to solve for surface luminance and summing for the 2p patches (to account for non horizontal receptors): $E_o = \sum_{i=1}^{2p} \left(L^* \Phi \omega \tau \cos \xi \right)_j$.

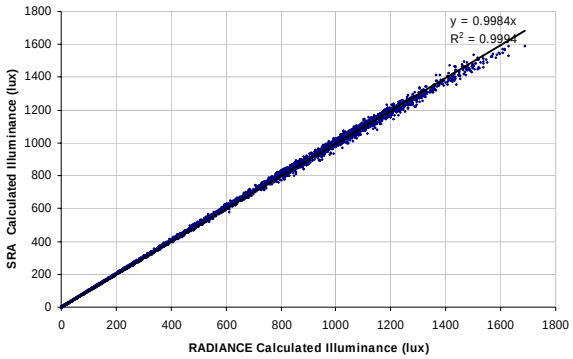

Figure 3 Comparisons between the SRA and RADIANCE for the hypothetical canyon discussed above, for a single point within a room extruded from a south facing façade.

Figure 3 compares results from calculations of these two sources of illumination using the SRA and RADIANCE.

Further details concerning the calculation of sky and externally reflected light as well as the use of the BRS split flux equation for internally reflected light can be found in Robinson and Stone (2005a). Concerning the latter however, comparisons with RADIANCE showed that the split flux approximation leads to significant deviations when illumination from windows is strongly directional (e.g. in the presence of sunlight) – though this tends not to be the case at low switching threshold illuminances of say ≤1 kLux, at which the approximation may be reasonable.

Nevertheless, to resolve the inaccuracies of internally reflected light prediction, a radiosity calculation was implemented[2]. For our purposes, the energy reflected to each internal surface element by every other element, is given by a slightly modified form of the standard radiosity equation:

$$E_{j,ref} = \sum_{i=1}^{n} f_{j \to i} \rho_i E_{gi} \qquad \ldots[5]$$

Where $E_{j,ref}$ is the light reflected to internal surface j from all of the other internal surfaces, $f_{j \to i}$ is the form factor from internal surface j to internal surface i, E_{gi} is the global illuminance of internal surface i, and n is the total number of internal surfaces. The illuminance due to internally reflected light at the measurement point E^* is then:

$$E^* = \sum_{i=1}^{n} \rho_i f_i^* E_{gi} \qquad \ldots[6]$$

Where n is the number of internal room surfaces and f_i^* is the form factor from the measurement point to internal surface i. This is somewhat standard. However, following a series of experiments to improve the efficiency with which matrix formulations of these radiosity equations are solved, a procedure was identified which yields a solution in only slightly more computations than the split flux equation involves (see Robinson and Stone, 2005b). The accuracy of the solution though,

[2] In fact improvements to the split flux equation were also tested. A further term was added, so that incoming energy incident on walls was apportioned the correct reflectance and a radiosity/split-flux hybrid was tested, for better resolution of the first-reflected flux. However, the extent of residual interior anisotropy for subsequent reflections (in sunlit situations) led to this approach being abandoned in favour of rapid radiosity calculations.

is dependent upon that with which the incident flux at each patch is calculated as well as the number of these patches; and this comes at a pre-processing cost.

Several methods for allocating the incoming flux were tested. Of these a good compromise between accuracy and computational cost was a method of projecting the shape of windows into the room, along the opposite vector of the light source of interest (patch or sun) – which is treated as though located at infinity, to each internal surface element. The flux is then apportioned according to the proportion of projected parallelogram(s) that is taken up by a given surface element. The simplifying assumption here then is that the energy incident at window planes is uniformly distributed.

A sensitivity study suggests that for simple rooms it is adequate simply to split vertical surfaces horizontally at the calculation point height and then all surfaces into front and rear halves, Figure 4.

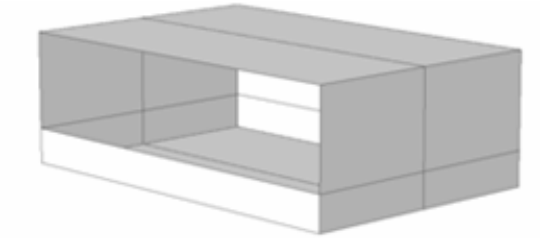

Figure 4 Surface splitting of simple room adopted for comparisons.

For the purposes of comparison however, a scenario avoiding pre-processing simplifications has been composed (Figure 5).

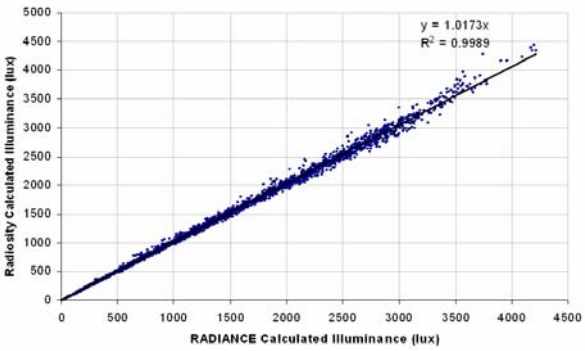

Figure 5 Internally reflected light as calculated by the SRA with a full radiosity simulation (explicit obstruction view factor and ray traced solar visibility computation from each internal surface), compared with RADIANCE.

The scatter in results is due predominantly to the spatially insensitive way with which external surface luminance is calculated[3]. As noted above, the recommended method of light source projection introduces additional errors, but these are reasonable (slope error < 2%), given the computational efficiency: for a scene with 1018 rooms, each with 15 internal surfaces, the total run time for annual hourly simulations on a moderately quick PC is <7s.

LONGWAVE RADIATION

The net long wave irradiance I_L (W) at a surface s of area A and emissivity ε can be solved (Clarke, 2001) by representing the external environment as an equivalent temperature T^* (K), so that $I_L = \varepsilon A\theta\left(T^{*4} - T_s^4\right)$ where θ is the Stefan-Boltzmann constant (~5.67E-8 $Wm^{-2}K^{-4}$) and T^* is the sum of the products of contributing source view factor and temperature. Using our knowledge of the urban scene then, our effective temperature is:

$$T^{*4} = \frac{1}{\pi}\left(T_{sky}^4 \sum_{i=1}^{145}\left(\Phi\sigma\cos\xi\right)_i + \sum_{j=1}^{290}\left(\Phi\omega\cos\xi T^4\right)_j\right) \quad \ldots[7]$$

A comprehensive study by Skartveit et al (1996) compared long wave irradiance predictions from 34 empirical formulae to those from MODTRAN – an extensively tested first principles program simulating the range of absorption and emission processes – and to measurements, to identify those with the widest range of applicability. From this it was concluded that the formula due to Berdahl and Fromberg (1982), which expresses cloud free emittance as a linear function of dew point temperature (T_d) [8], performs adequately over a wide range of temperature and humidity.

$$\varepsilon_0 = I_{L\downarrow} \big/ \theta T_{sky}^4 = 0.741 + 0.00062 T_d \quad \ldots[8]$$

The increase in atmospheric emittance beyond its cloudless value ε_0 due to clouds, which after Berdahl and Martin (1984) can be phrased as $\left(\varepsilon - \varepsilon_0\right)/\left(1-\varepsilon_0\right)$, is a function of cloud cover, emittance, base height and temperature gradient. Fortunately, in the absence of the relevant measurements, this emittance increase can be expressed to a good approximation (Skartveit et al, 1996), as: $\left(\varepsilon - \varepsilon_0\right)/\left(1-\varepsilon_0\right) \approx n^{2.5}$ given the fractional cloud cover n ($n = C/8$, where C is cloud cover in Oktas)].

Now, considering: (i) the intrinsic uncertainties in estimating sky temperature [particularly at night];

[3] By removing obstructions the slope error reduces to *c.*0.55%, there is very little scatter and $r^2 > 0.999$.

(ii) that temperature difference between a given surface and the sky will tend to exceed that between surfaces; and (iii) the uncertainty in calculating a local convective heat transfer coefficient; a pragmatic approach to the temperature of the *j*th obstruction for the longwave exchange term in [7] suggests the use of results from the previous time step. A future implementation, in which these sources of error are contained, might usefully consider simultaneous solution of building energy and external longwave radiation exchanges.

On the basis that the short wave radiation model has been shown to closely match sky radiation predictions from a ray tracing program, it is reasonable to suggest that any error in long wave radiation exchange to the sky is due to sky temperature estimation; likewise for obstructions. Since we have no computationally efficient yet reliable basis for the estimation of either temperature, we have not attempted to compare predictions from this calculation either with some truth model or with some empirical dataset.

IMPLEMENTATION

The overall structure of the radiation model is shown in Figure 6. The first step in the solution process is the view factor calculation, the input to which is a description of the geometry of the scene describing the various surfaces and the locations of their vertices. The outputs from the view factor calculation are the view factors and solar visibility fractions for both internal and external surfaces.

The view factors are then used with the surface properties (e.g. diffuse reflectance) to construct the various matrices that are used as part of the main solution routine. The sky luminance distribution at each time step is also calculated in the pre-processing stage.

The main calculation then proceeds as follows for each time step:

- Calculation of short wave radiation exchange: the short wave radiation received at each surface due to the sun and the sky vault is calculated separately. These two contributions are then multiplied by the beam and diffuse luminous efficacies respectively (as given by the Perez sky model) to give the luminance of each surface, from which the sky and externally reflected illuminance is calculated.
- Calculation of the magnitude of internally reflected light for each room.
- Calculation of the long wave radiation exchange: the long wave radiation exchange calculation requires the temperatures of each of the external surfaces. This may be taken as that predicted by some thermal model at the previous time-step.

As mentioned earlier prediction results can be displayed by false-colouring surfaces. By way of final demonstration, results from predictions of annual solar irradiation from RADIANCE are compared with the SRA for a simplified geometric model of Canary Wharf in London, UK. For this model each surface, which has diffuse reflectance of 0.2, has been split in advance into ≤10m x 10m sub-surfaces for the SRA. From Figure 7 it is immediately apparent that the new model reproduces the variation in irradiation across surfaces in a complex urban scene that RADIANCE predicts.

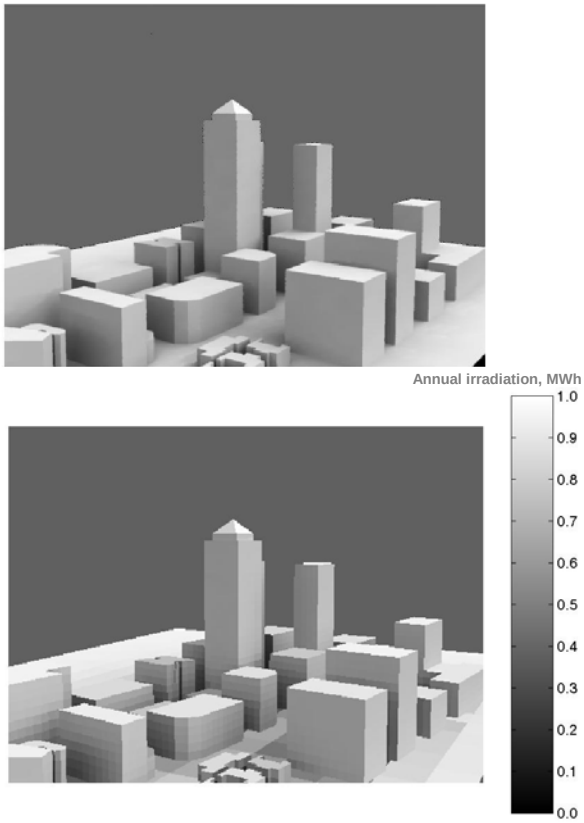

Figure 7 Predictions of annual solar irradiation throughout a simplified 3D model of Canary Wharf from RADIANCE (above) and the SRA (below) – based on surfaces of ≤10m x 10m[4].

This Canary Wharf model is composed of ~6 500 surfaces and for each the combined SRA solves for

[4] However, the ground is treated somewhat simplistically in this particular case (i.e. surface sizes are relatively large) since we are more concerned with building surfaces here.

hourly shortwave, visible and longwave radiation for a complete year in ~900s using a moderately quick PC (1GB RAM, 1.8GHz). Approximately 200s of this is taken up by view factor computations and ~700 by resultant processing. It is impractical to compare run time with RADIANCE, since this would involve ~19 500 separate hourly simulations for just visible and shortwave radiation. Our experience suggests that equivalent (though more accurate) results would take more than five orders of magnitude longer to produce using RADIANCE.

CONCLUSIONS

In representing aggregated occlusions to discrete patches of a vault as a patch view factor for which we define the dominant contributing occlusion, we have a basis for predicting energy exchange between both occluded and unoccluded regions of this patch and some point on a surface. In fact we may solve for successive exchanges between points on all surfaces and all occluded patches either iteratively or by matrix inversion, so that we have a new simplified radiosity algorithm (SRA). This SRA has been applied to predict short wave irradiance, interior illuminance and long wave irradiance. For the short wave and daylight applications, results have also been compared with the extensively tested ray tracing program RADIANCE. From this we conclude that:

- Results from the application of the SRA to solar radiation prediction compare well with those from the ray tracing program RADIANCE, with interpolation of hourly solar visibility profiles between adjacent months representing the principal source of error. The excellent agreement observed between the SRA and RADIANCE for diffuse-only simulations, confirms that the simplifications made in this SRA do not impair accuracy.

- Using predictions of beam and diffuse luminous efficacy, the SRA also predicts external illumination to a high degree of accuracy. Furthermore, use of a cumulative global sky radiance distribution facilitates rapid prediction of annual irradiation.

- By determining view parameters at points within (real or hypothetical) rooms the SRA is readily adapted to predict interior illuminance due to the sky and external reflections. Comparisons with RADIANCE suggest similar accuracy as for external illuminance / irradiance. Experiments to identify a high efficacy solution for internally reflected light suggest the use of a radiosity solution for a coarsely discretised room, using a light source projection technique for incoming flux allocation. Good agreement with RADIANCE is once again observed, at a fraction of the computational cost.

- The view parameters from the SRA have been used to calculate an effective temperature that describes the external scene for each exposed surface. This has been used to predict surface long wave irradiance. However, there are several important sources of error: (i) sky temperature, (ii) local surface convective heat transfer coefficient, (iii) asynchronous solution of building and external surface exchange. Future improvements to (i) and (ii) may warrant a future synchronous building/surface solution to reduce prediction errors.

- Using a moderately quick PC (1GB RAM, 1.8GHz) the SRA predicts hourly solar irradiance, internal illuminance at two points and long wave irradiance for an urban scene composed of >1 000 surfaces in *c*. 90 seconds.

The proposed SRA is incorporated within a new prototypical sustainable urban neighbourhood modelling tool (SUNtool) as part of an EC-funded research project. This algorithm is amenable for inclusion into standard computer programs that require the predicted radiation quantities as an input - such as dynamic simulation programs. Further applications of the SRA may include noise transfer and integration within a thermal microclimate model for local temperature prediction.

ACKNOWLEDGEMENTS

The funding for Project SUNtool by the European Commission's DG TREN is gratefully acknowledged. Thanks also to Christian Roecker and two anonymous referees for their helpful comments on drafts of the paper.

REFERENCES

Berdahl, P. Fromberg, R. (1982), The thermal radiance of clear skies, Solar Energy 29(4), pp299-314.

Berdahl, P. Martin, M. (1984), Emissivity of clear skies, Solar Energy 32(5), pp663-664.

Clarke J. A. (2001), Energy simulation in building design: Butterworth Heinemann 2nd Ed.

Compagnon, R., Solar and daylight availability in the urban fabric, Energy and Buildings, 36(4), p321-328.

Population reference bureau (2005): http://www.prb.org/Content/NavigationMenu/PRB/

Educators/Human_Population/Urbanization2/Patterns_of_World_Urbanization1.htm

Perez, R., Ineichen, P., Seals, R., Modelling daylight availability and irradiance components from direct and global irradiance, Solar Energy 44(5) p271-289, 1990.

Perez, R Seals, R Michalsky, J, All-weather model for sky luminance distribution – preliminary configuration and validation, Solar Energy 50(3), 235-243, 1993.

Robinson, D., Stone, A. (2004a), Solar radiation modelling in the urban context, Solar Energy, 77(3) 2004, p295-309.

Robinson, D. Stone, A. (2004b), Irradiation modelling made simple: the cumulative sky approach and its applications, Proc PLEA 2004, Eindhoven Netherlands, 20-22nd September, Vol. 2 pp1255-1259.

Robinson, D., Stone, A. (2005a), Internal illumination prediction based on a simplified radiosity algorithm, Solar Energy (in press).

Robinson, D., Stone, A. (2005b), A simplified radiosity algorithm for general urban radiation exchange, Building Services Engineering Research and Technology (in press).

Tregenza P, Sharples S. Daylighting Algorithms. ETSU Report S1350, 1993.

Skartveit, A. Olseth, J.A. Czeplak, G. Rommel, M. (1996), On the estimation of atmospheric radiation from surface meteorological data, Solar Energy, 56(4), pp349-359.

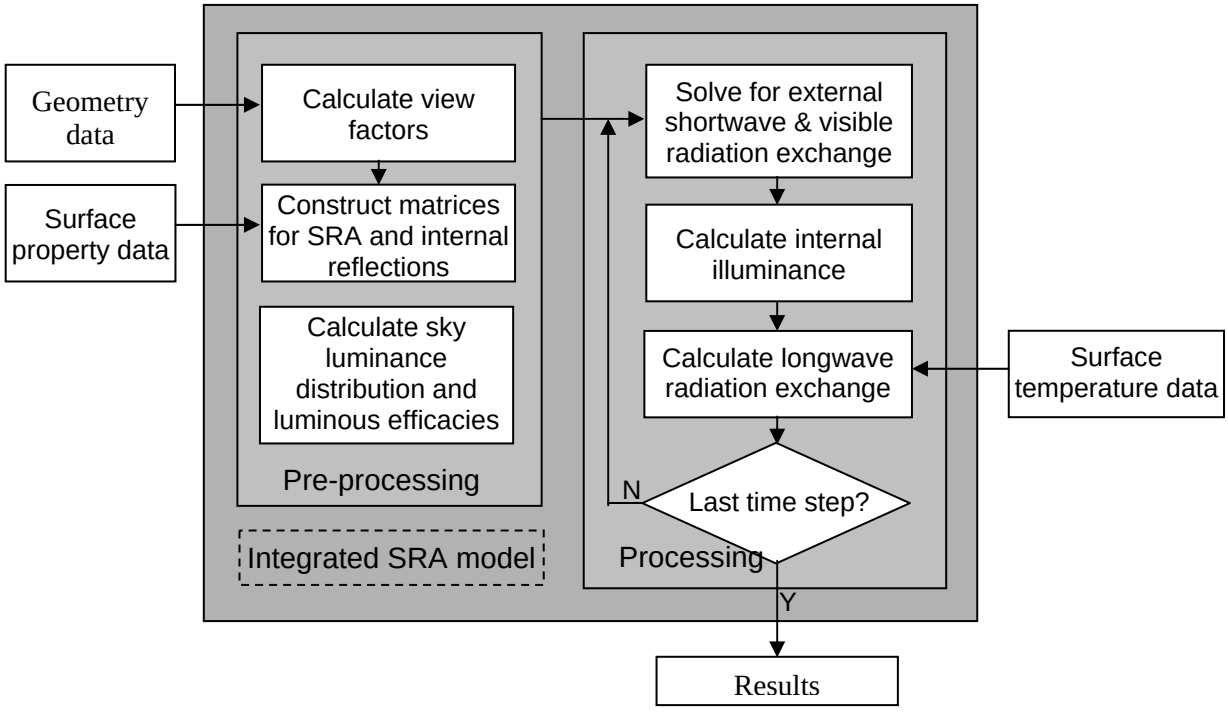

Figure 6 Schematic diagram illustrating the radiation model solution process.

NOMENCLATURE

A	Area, m^2	L	Luminance, $lm.m^{-2}.Sr^{-1}$
C	Cloud cover, Okta	n	Fractional cloud cover
E	Illuminance, Lux	R	Radiance, $W.m^{-2}.Sr^{-1}$
f	Form factor	T	Temperature, K
I	Irradiance, Wm^{-2}		

Greek:

ε	Emissivity, emittance
θ	Stefan-Boltzmann Constant, $W.m^{-2}.K^{-4}$
γ	Altitude, rad
Φ	Solid angle, Sr
ξ	Angle of incidence, rad
ρ	Reflectance
τ	Transmittance
ℓv	relative luminance, $lm.m^{-2}.Sr^{-1}$
σ,ω,φ,Ψ	View factors corresponding to sky, obstruction, room and solar sources respectively.

Subscripts/superscripts:

b	Beam
d	Diffuse; dewpoint
g	Global
h	Horizontal
L	Longwave
n	Normal
β	Tilted
*	Effective; dominant

APPENDIX 1

The inclusion of reflections means that the irradiance of a particular surface potentially depends on the radiance / luminance of up to 290 different surfaces – solving for reflection from each patch.

A convenient way of solving for this reflection is to formulate the problem as a matrix equation and solve by inversion. For this we can write that $\underline{I_d} = A\underline{I_g} + B\underline{R}$; where $\underline{I_g} = \underline{I_d} + \underline{I_b}$ is a vector listing the global irradiance on each surface, and $\underline{R}$ a vector giving the radiance of each sky patch.

Rearranging:

$$\underline{I_d} = (I - A)^{-1}(A\underline{I_b} + B\underline{R}) \quad \ldots[A1.1]$$

The matrix *A* is square and describes how the direct component of irradiance falling on each surface is eventually distributed around the *n* surfaces in the scene (entry (*i*,*j*) in the array describes the proportion of direct insolation on surface *j* that is reflected to surface *i*):

$$A = \begin{bmatrix} \frac{\rho_1 k_{1,1}}{\pi} & \frac{\rho_2 k_{1,2}}{\pi} & \cdots & \frac{\rho_n k_{1,n}}{\pi} \\ \frac{\rho_1 k_{2,1}}{\pi} & \ddots & & \vdots \\ \vdots & & \ddots & \vdots \\ \frac{\rho_1 k_{n,1}}{\pi} & \frac{\rho_2 k_{n,2}}{\pi} & \cdots & \frac{\rho_n k_{n,n}}{\pi} \end{bmatrix} \quad \ldots[A1.2]$$

where ρ_i is the reflectance of surface *i*, and $k_{i,j}$ describes a scaling factor for the effect of the energy reflected from surface *j* to surface *i*. If surface *j* obstructs *m* sky patches when viewed from surface *i*, denoted by $x_1, x_2, ..., x_m$, then:

$$k_{i,j} = \sum_{k=1}^{m} \Phi_{i,x_k} \left(1 - \sigma_{i,x_k} - \sigma_{self,x_k}\right) \cos \xi_{i,x_k} \quad \ldots[A1.3]$$

where σ_{i,x_k} is the view factor from surface *i* to sky patch *xk* and Φ_{i,x_k} is the solid angle of sky patch *xk* from surface *i*.

Matrix *B* describes the contribution from each sky patch (of unit radiance) to the irradiance received by each surface within the scene:

$$B = \begin{bmatrix} \Phi_{1,1}\sigma_{1,1}\cos\xi_{1,1} & \Phi_{1,2}\sigma_{1,2}\cos\xi_{1,2} & \cdots & \Phi_{1,p}\sigma_{1,p}\cos\xi_{1,p} \\ \Phi_{2,1}\sigma_{2,1}\cos\xi_{2,1} & \ddots & & \vdots \\ \vdots & & \ddots & \vdots \\ \Phi_{n,1}\sigma_{n,1}\cos\xi_{n,1} & \Phi_{n,2}\sigma_{n,2}\cos\xi_{n,2} & \cdots & \Phi_{n,p}\sigma_{n,p}\cos\xi_{n,p} \end{bmatrix} \quad \ldots[A1.4]$$

The matrices $(I - A)^{-1}A$ and $(I - A)^{-1}B$ need only be computed once for any given geometry. Therefore at each time step once the direct component of irradiance has been solved for, only two matrix multiplications and an addition are required to solve for the diffuse component.

Note that by replacing $\underline{I_x}$ by $\underline{E_x}$ and $\underline{R}$ by $\underline{L}$ in A1.1 we have predictions of surface illuminance.

Finally, re-writing the expression for the vector $\underline{I_d}$ so that $\underline{I_d} = A'\underline{I_g} + B\tau'\underline{R}$ we may solve for the irradiance transmitted through a surface of glazed fraction $f\underline{I_g} = f\left(\underline{I_d} + \underline{I_b}\tau\right)$. For this, entry *i,j of* τ' describes the transmittance of the *i*th surface from the *j*th patch and $k_{i,j}$ of A' includes this transmittance (now referring to the *k*th patch):

$$k_{i,j} = \sum_{k=1}^{m} \Phi_{i,x_k} \left(1 - \sigma_{i,x_k} - \sigma_{self,x_k}\right) \cos \xi_{i,x_k} \tau_k \,.$$